



Efficient one-cycle affinity selection of binding proteins or peptides specific for a small-molecule using a T7 phage display pool

Yoichi Takakusagi^{a,†}, Kouji Kuramochi^{a,†}, Manami Takagi^b, Tomoe Kusayanagi^a, Daisuke Manita^a, Hiroko Ozawa^b, Kanako Iwakiri^b, Kaori Takakusagi^a, Yuka Miyano^a, Atsuo Nakazaki^b, Susumu Kobayashi^{b,*}, Fumio Sugawara^{a,*}, Kengo Sakaguchi^{a,*}

^a Department of Applied Biological Science, Faculty of Science and Technology, Tokyo University of Science, 2641 Yamazaki, Noda, Chiba 278-8510, Japan

^b Department of Medicinal and Life Science, Faculty of Pharmaceutical Sciences, Tokyo University of Science, 2641 Yamazaki, Noda, Chiba 278-8510, Japan

ARTICLE INFO

Article history:

Received 20 August 2008

Revised 19 September 2008

Accepted 20 September 2008

Available online 30 September 2008

Keywords:

Small-molecule-oriented T7 phage display

QCM

Self-assembled monolayer

One-cycle screen

Drug-like small-molecule

Synthetic ligand for FK506-binding protein

(SLF)

Irinotecan (Iri, CPT-11)

ABSTRACT

Here, we report an efficient one-cycle affinity selection using a natural-protein or random-peptide T7 phage pool for identification of binding proteins or peptides specific for small-molecules. The screening procedure involved a cuvette type 27-MHz quartz-crystal microbalance (QCM) apparatus with introduction of self-assembled monolayer (SAM) for a specific small-molecule immobilization on the gold electrode surface of a sensor chip. Using this apparatus, we attempted an affinity selection of proteins or peptides against synthetic ligand for FK506-binding protein (SLF) or irinotecan (Iri, CPT-11). An affinity selection using SLF-SAM and a natural-protein T7 phage pool successfully detected FK506-binding protein 12 (FKBP12)-displaying T7 phage after an interaction time of only 10 min. Extensive exploration of time-consuming wash and/or elution conditions together with several rounds of selection was not required. Furthermore, in the selection using a 15-mer random-peptide T7 phage pool and subsequent analysis utilizing receptor ligand contact (RELIC) software, a subset of SLF-selected peptides clearly pinpointed several amino-acid residues within the binding site of FKBP12. Likewise, a subset of Iri-selected peptides pinpointed part of the positive amino-acid region of residues from the Iri-binding site of the well-known direct targets, acetylcholinesterase (AChE) and carboxylesterase (CE). Our findings demonstrate the effectiveness of this method and general applicability for a wide range of small-molecules.

© 2008 Elsevier Ltd. All rights reserved.

1. Introduction

In forward chemical genetics, the T7 phage display method is a powerful tool that can be applied to the screening of small-molecule binding proteins or peptides.^{1–3} Using this method, in theory, drug-binding protein(s) or peptide(s) displayed on the T7 phage capsid can be effectively panned from a diverse range of proteins or peptides. However, the method relies on the chemically-defined binding strength *in vitro*, which does not always result in identification of the proteins responsible for bioactivity of the small-molecule *in vivo*. Thus, a rapid and reliable classification of small-molecule binding proteins from the ordered genome database is highly desirable. Using this information it should be possible to design a series of experiments to investigate the mode of action of the corresponding small-molecules.

Recently, we reported the establishment of an effective T7 phage display environment for small-molecules using a T7 phage display system and a cuvette type 27-MHz quartz-crystal microbalance (QCM) apparatus (Affinix Q, Initium, Tokyo, Japan).^{4,5} This novel approach overcomes the technical difficulties of a conventional screen using microplate or agarose beads and can be used for the rapid isolation of binding phage specific for small-molecule.^{4,5} Here, we further introduce a self-assembled monolayer (SAM) with multiple functions as a means of small-molecule attachment for the sensor chip.⁶ Two test molecules were used in this study: (i) a synthetic ligand for FK506-binding protein (SLF), an analog of the immunosuppressive agent FK506,⁷ and (ii) irinotecan (Iri, CPT-11), an anti-tumor camptothecin (CPT) derivative with clinical use.⁸ We verified selection from a natural-protein or random-peptide T7 phage pool. The latter approach also involves the use of receptor ligand contact (RELIC) software, a bioinformatics tool for phage display screening.⁹ This software system was developed using the concept that drug-like small-molecules with a rigid structure immobilized on a carrier appear to show weak interactions with peptide via surface–surface contacts against a continuous or discontinuous three- to five-amino-acid motif. Using a subset of small-molecule-selected random-peptides, with the peptide sequences arbitrarily selected from the

* Corresponding authors. Tel.: +81 4 7124 1501x6543 (S.K.), +81 4 7124 1501x3400 (F.S.), +81 4 7124 1501x3409 (K.S.).

E-mail addresses: kobayash@rs.noda.tus.ac.jp (S. Kobayashi), sugawara@rs.noda.tus.ac.jp (F. Sugawara), kengo@rs.noda.tus.ac.jp (K. Sakaguchi).

† Both authors equally contributed to this study.

unscreened parent pool, a significant change of amino-acid population, or the emergence of small-molecule-recognizing short stretches discernable by eye, can be statistically detected.^{2,9,10} By making use of this information and the subset of peptide sequences, further exploration of binding proteins from the database, as well as the validation of the peptide selection itself, is systematically feasible.⁹ The results of SLF and Iri in this paper demonstrate the effectiveness and general applicability of our strategy for screening of small-molecule binding proteins/peptides.

2. Results and discussion

2.1. Efficiency of SAM for SLF immobilization on the gold electrode surface of a sensor chip

To date, SAM has been reused as an immobilization scaffold to facilitate directed orientation and accumulation of the substrate on a gold (Au) surface.^{6,11} Using SLF^{7,12–14} as a candidate small-molecule, we initially synthesized the SLF derivative as shown in Scheme 1 and Figure 2A. The molecule comprises four units: (i) sulfide bond for chemisorption on the gold electrode surface of the sensor chip via thiol–Au interactions, (ii) a C11 alkyl chain¹⁵ for accumulation of the SLF molecule on the gold, (iii) diethylene glycol (DEG) for reducing the non-specific binding (mainly via hydrophobic interaction) with the gold surface or linkers, and (iv) SLF to act as bait during screening.

Using this synthetic molecule, we can attain one-step immobilization of SLF on a gold electrode surface of QCM sensor chip. SLF derivative was dissolved in 75% ethanol, dropped onto the gold electrode and then incubated for 16 h under a humid and shaded atmosphere at room temperature, which resulted in the formation of SLF-SAM on the gold electrode surface. After washing the surface of the electrode, the sensor chip was placed in the QCM apparatus using a buffer filled cuvette. The QCM sensor was then fully stabilized. To validate SAM immobilization, His-tagged FKBP12 was injected into the cuvette and the frequency changes that occurred upon binding to the immobilized SLF were monitored. Figure 2B shows the resulting sensorgram that was obtained by monitoring the interaction after injection of His-tagged FKBP12 at the indicated concentration. His-tagged FKBP12 showed a clear frequency decrease upon binding to SLF immobilized as SAM layers on the gold electrode surface (Fig. 2B, red line). By contrast, a less dramatic frequency change was detected during avidin–biotin immobilization using biotinylated SLF (SLF-bio, Fig. 2A) (Fig. 2B, black

line). From kinetic analysis using AQUA ver1.5 software (Initium Inc.), the K_D value was 15–19 nM, which is consistent with previously reported data.^{13,14} The B_{max} (100% binding ratio) of FKBP12 to immobilized SLF was 187–231 Hz (5.6–6.9 ng) in the case of SAM immobilization, whereas 58–77 Hz (1.7–2.2 ng) was calculated from the data obtained by avidin–biotin immobilization. These results indicate that the amount of active SLF molecule immobilized by SAM is at least threefold greater than is immobilized by avidin–biotin (Fig. 2C). Thus, the effectiveness of SAM immobilization over the avidin–biotin method is clear, at least using the QCM apparatus.

2.2. One-cycle affinity selection of T7 phages exhibiting preferential affinity for SLF from a natural-protein T7 phage pool

We next applied this SLF-SAM to a T7 phage display screen. When an aliquot of plaque forming units (pfu) of a freshly prepared natural-protein T7 phage pool was injected into the cuvette, a frequency change was detected (Fig. 3A). After monitoring the interaction for 10 min, the sensor chip was detached from the device. The genomic DNA of SLF-binding phage on the gold electrode surface was recovered using the host *Escherichia coli* (BLT5615) solution and amplified. A short interaction time (10 min) was sufficient to recover and amplify the bound phage, which showed lysis of the host *E. coli* after 30 min incubation at 37 °C. Sixteen phage particles were arbitrarily extracted from the resulting T7 phage solution and the enrichment was analyzed by sequencing the DNA encoding the fusion protein of the phage capsid. The T7 phage display screen using SLF-SAM and QCM resulted in clear detection of T7 phage whose capsid fusion protein corresponded to FKBP12, which was included at a rate of 10 out of 16 phage isolates (Fig. 3B, ●). In addition, three shorter peptides (Fig. 3B, ▲/16, ■/16, ◆/16), which included an amino-acid sequence similar to the proposed SLF analog-binding site within FKBP12 (Supplementary Fig. 1) adventitiously generated by the random primer strategy, were also isolated.^{4,16} Repeated cycles of screening tended to bias phage distribution in terms of the growth characteristics of each phage and lead to poor reproducibility. However, our methodology does not require multiple rounds of screening.

A conventional phage display protocol involves repeated cycles of screening in order to enrich for phage particles that specifically bind to the bait. Technically, an input of 10^9 – 10^{10} pfu/ml of parent phage pool is required because of the detection limit, which also

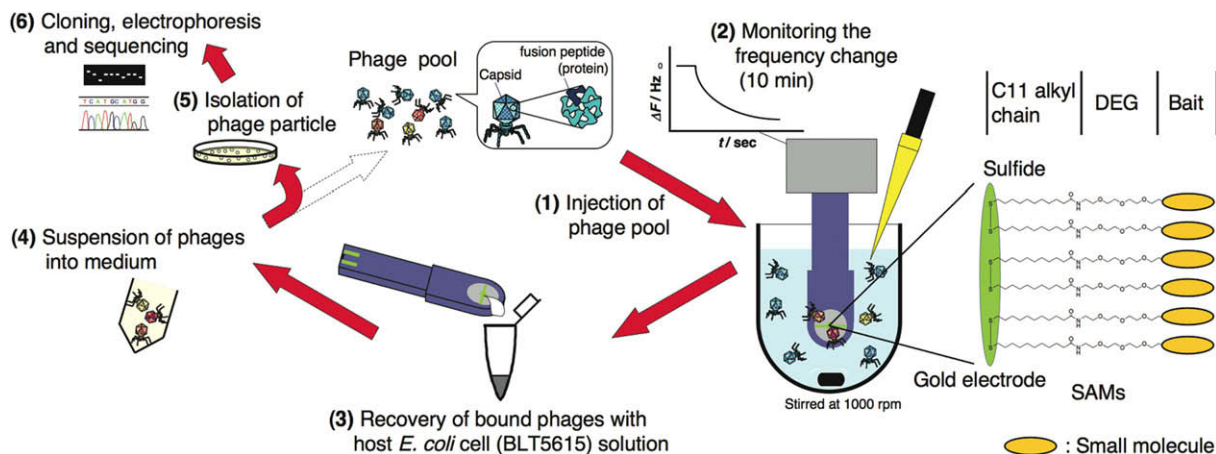
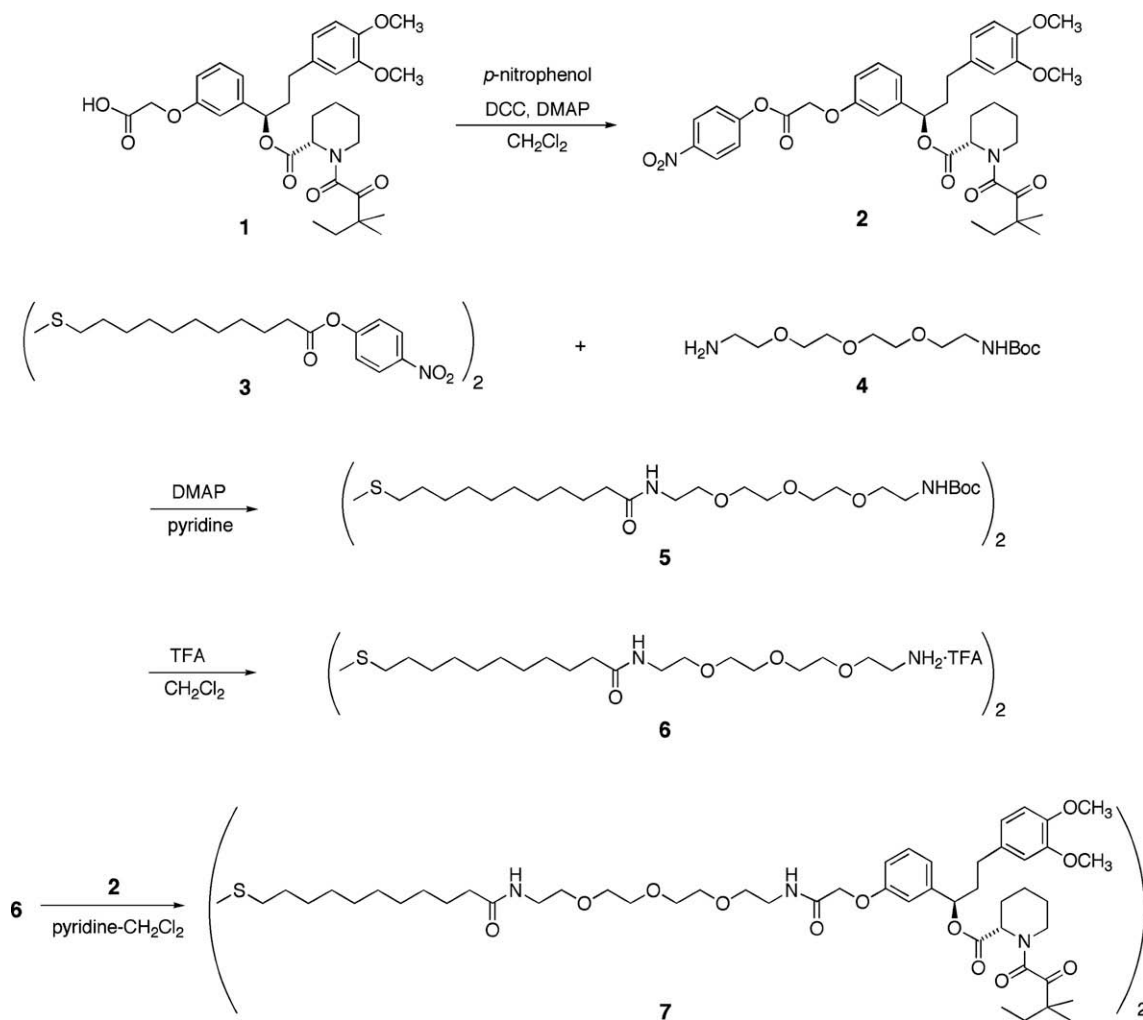


Figure 1. Schematic representation of a T7 phage display screen for drug-like small-molecule using a self-assembled probe and a cuvette type QCM apparatus. (1) An aliquot of T7 phage pool is injected into a cuvette containing saline solution stirred at 1000 rpm. (2) The frequency change that occurs upon binding of the phages to a target of interest immobilized by SAM onto the gold electrode is monitored in real time. (3) The bound phages are recovered using host cell (*E. coli* BLT5615, Novagen) solution. (4) The resulting solution is suspended into another medium. (5) An aliquot (10–100 plaques) of the recovered phage is isolated. (6) The capsid gene-coding region of each phage is cloned and analyzed by agarose gel electrophoresis followed by DNA sequencing. Using this platform, repeated rounds of selection is not required.



Scheme 1. Synthesis of SLF derivative.

increases the background of non-specifically binding phage particles. However, the high level of sensitivity of the QCM sensor combined with the efficient SAM immobilization procedure allows the parent phage pool to be reduced to 10^7 pfu/ml. Hence, there is a stochastic reduction in the occurrence of non-specifically bound phage in this case (Fig. 3B). Consequently, the total number of phage recovered from the gold electrode surface after an interaction period of 10 min is reduced to 10^2 – 10^3 pfu (data not shown) compared with 10^5 – 10^6 pfu using a conventional platform. Thus, our novel screening procedure enables the efficient identification of phage particles that bind to small-molecules. In particular, our method enhances the chances of a real-binding sequence emerging from the screen (typically, 10–100 of plaques are arbitrarily picked for sequencing) (see Fig. 1 (5 and 6)). For example, in the present screen we successfully isolated an FKBP12-displaying phage by sequencing only 16 phage particles. Thus, providing the SAM derivative can be synthesized, our phage screening procedure using a QCM device is readily applicable to any small-molecule of interest.

2.3. One-cycle affinity selection of T7 phages exhibiting a preferential affinity for SLF from a random-peptide T7 phage pool

The successful identification of FKBP12-displaying T7 phage in a one-cycle procedure from a natural-protein T7 phage pool using SLF-SAM was helped by the fact that the FK506 or SLF-binding site is located at the surface of FKBP12. By contrast, there are many

cases where immobilization of a small-molecule may render it inaccessible to the target protein binding site,^{4,5} or where the target protein itself cannot be displayed on a capsid because of problems of misfolding, low solubility or abundance. Taking these factors into consideration, we constructed a 15-mer random-peptide T7 phage pool and applied it to our screening platform. Use of the phage pool enables identification not only of a lock-and-key or induced-fit type interaction for a disordered flexible loop but also the small-molecule binding site located on a protein.^{1,2} Moreover, the resulting small-molecule-selected peptides having uniform length can conveniently be subjected to RELIC software, a bioinformatics tool for elucidation of the phage display screen.⁹

In this experiment, using the same procedure as for the natural-protein T7 phage pool, a subset of 15-mer peptides were obtained after four sets of individual one-cycle screens with only 10 min of monitoring (Fig. 4A and B). These peptides displayed a distribution of amino-acids that had clearly changed by comparison with that of the parent T7 phage pool (Supplementary Fig. 4B). In addition, there are many continuous or discontinuous amino-acid motifs in the 35 selected peptides calculated by MOTIF1 (Supplementary Fig. 5) and MOTIF2 program (data not shown) in RELIC software, which are not readily discernable by manual inspection alone. Meanwhile, subsequent analysis of the selected peptides showed a high degree of similarity with a part of SLF analog-binding site within FKBP12(F37V) (Fig. 4C–F),^{12,17} as elucidated using HETERO-align program in RELIC software.⁹ A similarity plot of 35 peptides along with the entire sequence of FKBP12(F37V) is shown in

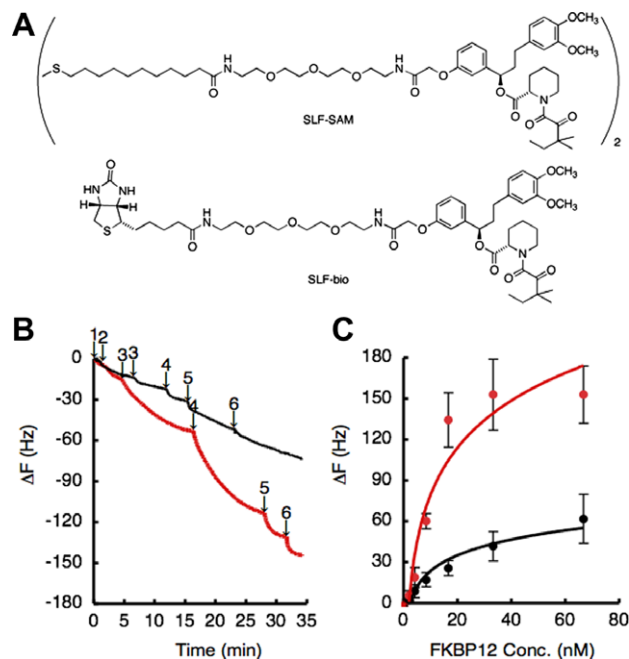


Figure 2. Validation of immobilization efficiency by SAM. (A) Structure of SLF derivative forming SAM and SLF-bio. (B) A representative QCM sensorgram obtained by monitoring the binding of His-tagged FKBP12 to an SLF-immobilized gold electrode surface of a sensor chip. The SLF-immobilized ceramic sensor chip generated by SAM (red line) or biotin-avidin interaction (black line) was individually attached to the QCM apparatus and the frequency decrease was monitored after injecting 8 μ l of each sample (1:2 μ M, 2:4 μ M, 3:8 μ M, 4:17 μ M, 5:33 μ M, 6:67 μ M) into a cuvette containing 8 ml of buffer. (C) Non-linear plot of frequency change (ΔF) against various final concentrations (nM) of His-tagged FKBP12 in the cuvette. Data are means \pm SD of three independent experiments. SLF-SAM: red line, SLF-bio: black line. AQUA ver1.5 software (Initium Inc.) was used to determine the kinetic parameters. 1 Hz = 30 pg.

Figure 4B, which was calculated using a modified BLOSUM62 score. A similarity plot of 103 peptides (arbitrarily selected from the unscreened parent pool) along with the entire sequence of FKBP12(F37V) was subtracted from the data before plotting. As a result, this plot clearly pinpointed 38D, 92I, and 98L in FKBP12(F37V) as residues of maximal similarity score (Fig. 4C). These three residues had previously been demonstrated to be contact sites for SLF analogs during the binding process. As shown in Figure 4F, several other amino-acids, including 37V, 83Y, 88H, 91I, and 100F (highlighted in color), were also found to be relatively high- or low-affinity sites of contact, consistent with previous binding experiments.^{12,17}

By contrast, 27Y, 47F, 56V, 57I, and 60W were not assigned as likely SLF-binding sites, even though contact of these amino-acids had previously been demonstrated (Fig. 4F, blue). We reasoned that these anomalous results could be due to a disturbance during the selection process caused by the SAM linker, introduced at the carboxylic group in SLF and aligned with high-density on the gold electrode. Indeed, the highlighted amino-acids are all located at the opposite side of the carboxylic group (Scheme 1 and Fig. 4E and F). Alternatively, as a result of technical limitations, it is likely that there are a number of sequences absent in the parent phage pool. The variation of phages possible in this system is up to 10^8 pfu, although the theoretical number of whole 15-mer peptides is 20^{15} ($\approx 3.28 \times 10^{19}$). Thus, the peptide anticipated to be selected by SLF (i.e., pinpoint 27Y, 47F, 56V, 57I, and 60W) may not have been included in the phage pool. Rigorous inspection of the SLF-binding site together with the identification of target protein is feasible, even though the variation of random-peptide T7 phage pool is $\sim 10^8$. Furthermore, unlike target identification from a natural-

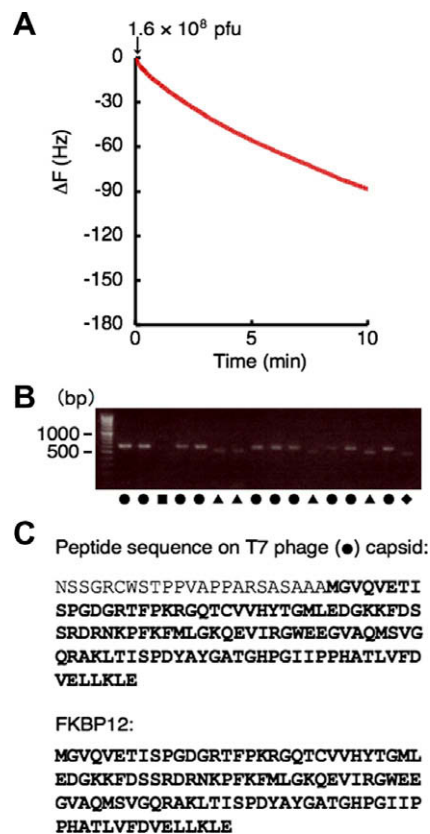


Figure 3. Detection of phage binding to an SLF-SAM-immobilized gold electrode surface of a sensor chip after injection of a natural-protein T7 phage pool. (A) The SLF-immobilized ceramic sensor chip generated by SAM was first attached to the QCM apparatus. After injecting a natural-protein T7 phage pool at the indicated concentration, the frequency decrease was monitored for 10 min. (B) Enrichment of T7 phage particles within the resulting solution. The binding phages on SLF-SAM-immobilized gold electrode were recovered and amplified using *E. coli* (BLT5615) solution. Sixteen T7 phage particles were arbitrarily extracted from the resulting solution and then analyzed by PCR amplification of the DNA encoding the fusion protein. Agarose gel electrophoresis of the PCR products followed by DNA sequence analysis allowed the 16 clones to be classified into four groups (10/16, ●; 4/16, ▲; 1/16, ■; 1/16, ◆). (C) (Poly)peptide sequence that was displayed on the T7 phage (10/16, ●). This sequence fully corresponds to that of FKBP12.

protein T7 phage pool or protein extract, this approach is independent of the physicochemical properties or abundance of the target protein.

2.4. General applicability of one-cycle affinity selection of T7 phages exhibiting preferential affinity for small-molecules

To further demonstrate the general applicability of this screening procedure, we attempted another experiment using Iri (Scheme 2). Iri is a derivative of camptothecin (CPT), a natural product from the Chinese bush *Camptotheca acuminata*, with potent anti-tumor activity.⁸ This water-soluble compound is a pro-drug with clinical use that is metabolized to the active SN-38 by liver carboxylesterase (CE) and acts as a topoisomerase I (top I) inhibitor.¹⁸ Recently, acetylcholinesterase (AChE) has been reported as an alternative direct target of Iri, and the mechanism of docking between the two molecules has been solved by X-ray crystallography.¹⁹ Using our screening procedure (Fig. 5A), we obtained 29 peptides (Fig. 5B) and successfully pinpointed several amino-acid residues (121Y, 225Q, 290F, 327E, 440H, and 442Y) overlapping part of the Iri-binding site in AChE (Fig. 5C–E).¹⁹ Likewise, the identical subset of peptides also indicated several amino-acids (99E, 100L, 252L, 305L, 387I, and 474V) (Fig. 6A) in

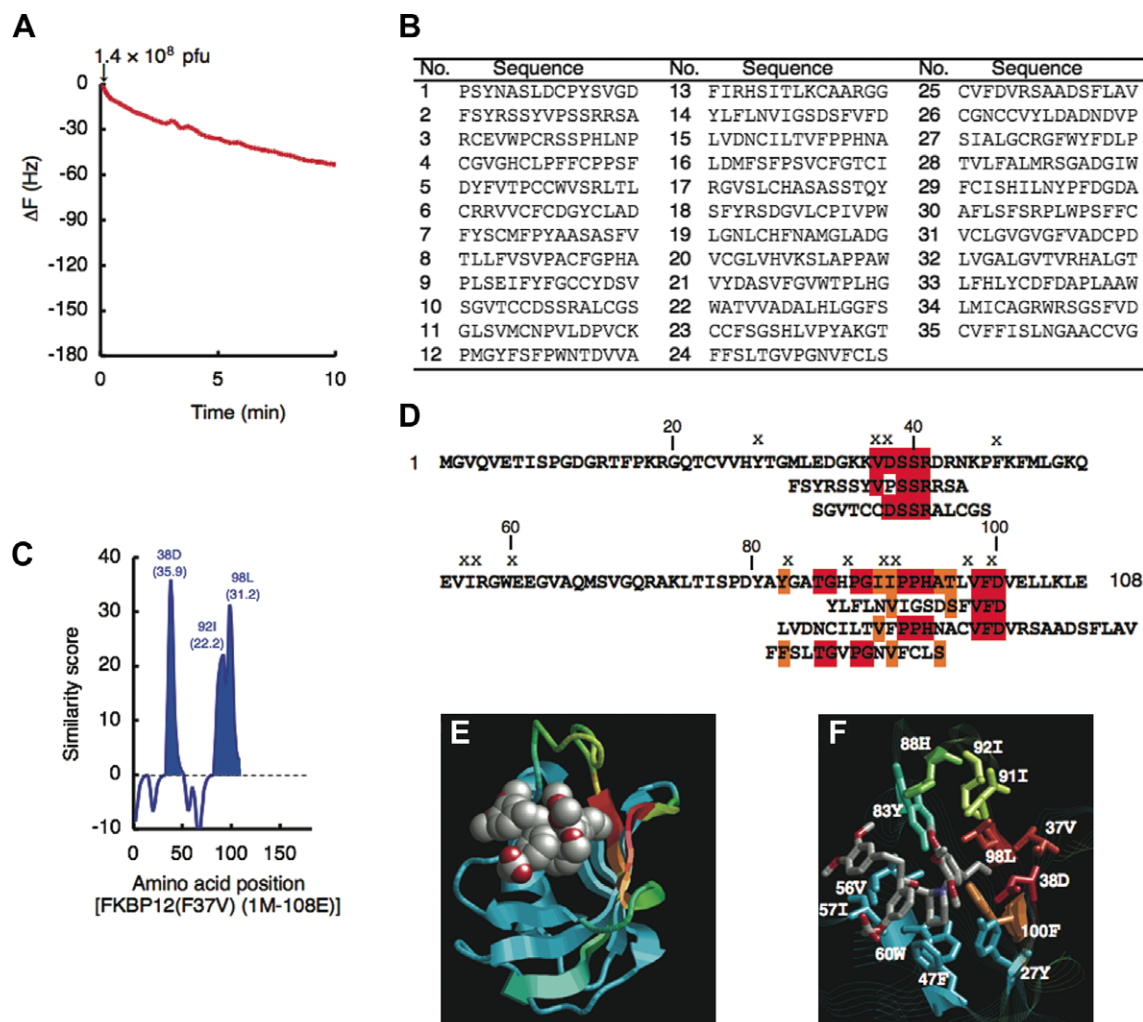


Figure 4. Detection of phage binding to SLF-SAM on the gold electrode after injection of a random-peptide T7 phage pool. (A) A representative sensorgram. Experiments were carried out according to the same procedure with natural-protein T7 phage pool. (B) SLF-SAM-selected 15-mer peptide sequence after four sets of individual one-cycle screens. T7 phage particles were arbitrarily extracted from the resulting solution and then analyzed by PCR amplification of the DNA encoding the fusion peptide. The PCR products were then sequenced. (C) Similarity scores for the sequence of FKBP12(F37V) (1M-108E) against the sequences of 35 peptides selected for affinity to SLF-SAM calculated using HETEROalign program in RELIC software (<http://relic.bio.anl.gov/index.aspx>). The similarity scores of random-peptides chosen without affinity selection (Supplementary Fig. 2) have been subtracted from these scores to remove pool bias. The maximal similarity score was observed for 38D (35.9), 92I (22.2) and 98L (31.2) (each peak is highlighted in blue). (D) Cluster diagram for the SLF-SAM-selected 15-mer peptide sequences in which each peptide is aligned to the input FKBP12(F37V) sequence at the position of maximal similarity. Residues exhibiting identity or similarity to the protein sequence are highlighted in red or orange. X indicates an amino-acid residue located within a distance of 5 Å from SLF analog-bound FKBP12(F37V). (E) Three structural models of SLF analog-FKBP12(F37V) complex (PDB ID: 1BL4). The peptide backbone of FKBP12(F37V) is shown in cartoon; SLF analog is shown in CPK. Oxygen in SLF analog is shown in red. Similarity is coded by color; red indicates the highest similarity and blue the lowest. (F) A close up view of the SLF analog-binding site rendered with RasMol with the amino-acid residues predicted to be involved in SLF-binding represented as a stick. SLF analog is shown in stick.

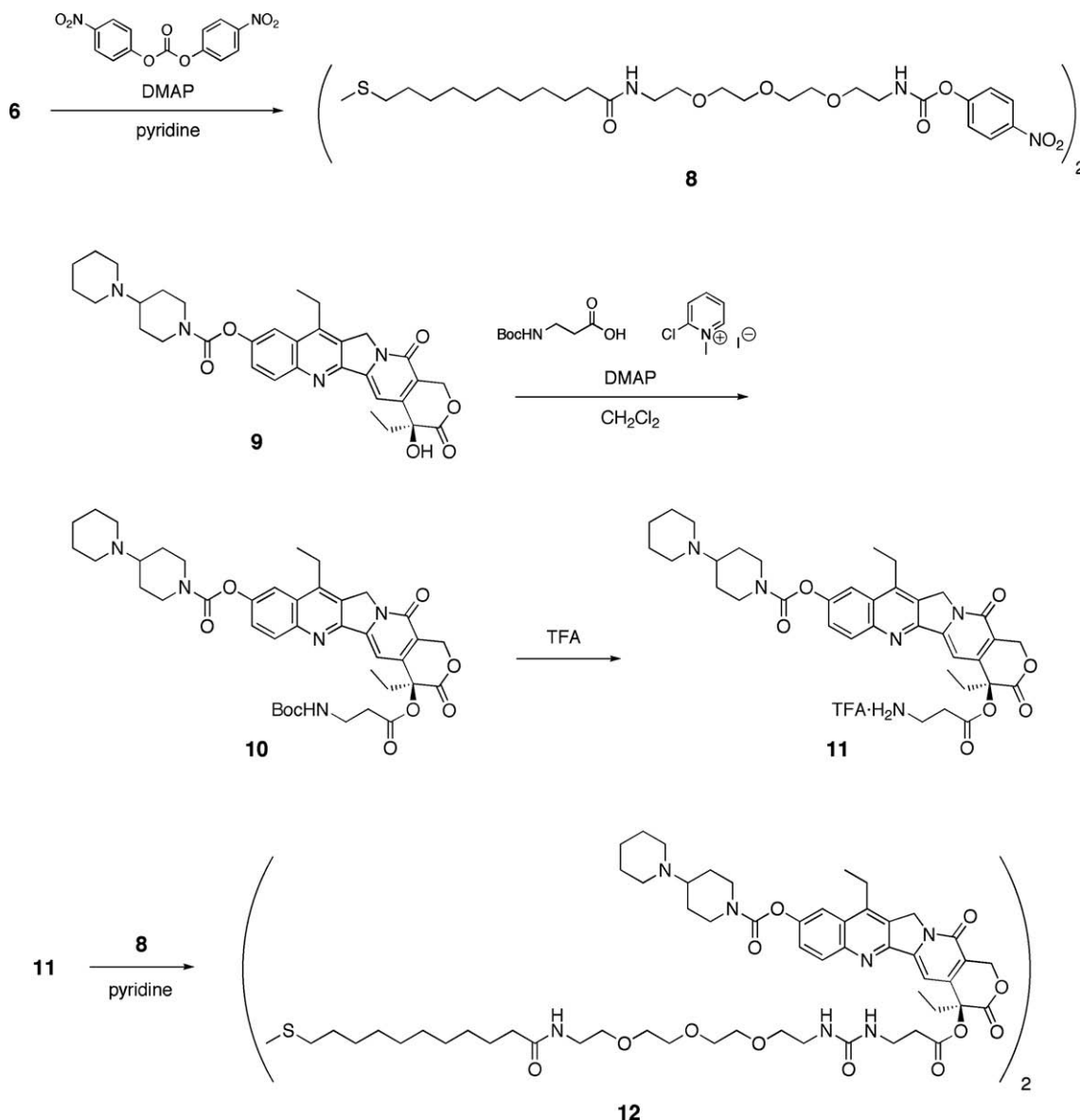
the vicinity of the catalytic triad (221S, 353E, and 467H) in CE, which potentially corresponds to the scaffold for Iri during the deesterification (Fig. 6B and C).²⁰ From our experimental data, together with the previous report, the likely location of each amino-acid during the Iri docking can be determined (see Fig. 6D). In our previous experiment using CPT-10-B, a portion of beta strand (210G-220E) on the opposite side of 474V was also identified,⁴ verifying the accuracy of this data. Unlike the case of AChE, docking between Iri and native CE may not be directly detected in either the X-ray or NMR structures because the enzymatic reaction is likely to proceed smoothly under the experimental conditions required for these methods. Nonetheless, our strategy, which depends on the primary peptide sequence, enables direct detection of the scaffold in the vicinity of the catalytic site.

However, part of the beta strand away from the well-defined Iri-binding site was also highlighted for both AChE (Fig. 5D) and CE (Fig. 6B). These highlighted residues can be regarded as false

positives or potential Iri-binding sites not involved in the bioactivity (generally categorized as “non-specific binding”). Furthermore, there are amino-acid residues in AChE, and perhaps in CE, known to be involved in Iri-binding that were undetected during our analysis. Our inability to select these residues could be due to problems associated with the linker or the limited size of the parent phage pool as discussed earlier for SLF. Thus, these amino-acids may be rendered detectable by altering the position of the introduced linker in Iri, increasing the number of Iri-selected peptides, or increasing the variation of the parent library to as close to the theoretical number as possible.

3. Conclusion

In summary, we have successfully established an effective small-molecule-oriented T7 phage display screen as a one-cycle



Scheme 2. Synthesis of Iri derivative.

method for identifying interacting species using both natural-protein and random-peptide T7 phage pools after an interaction time of only 10 min. By combining a QCM apparatus and SAM immobilization with T7 phage display, target discovery of various small-molecules can be effectively and universally accomplished. As a high-throughput screening platform, our method could dramatically facilitate the detection of T7 phage(s) that can bind to an immobilized small-molecule to validate the molecular interaction(s), even using a new bioactive compound or a functionally unknown target. We believe this methodology will contribute to the development of forward chemical genetics together with a range of other applications.

4. Experimental

4.1. Materials

The QCM apparatus (AffinixQ) and ceramic sensor chip were purchased from Initium Inc. (Tokyo, Japan). T7select10-3 OrientExpress™ cDNA Cloning System and pET28a(+) vector were from

Novagen (Madison, WI). Klenow DNA polymerase I was purchased from USB Corporation (Cleveland, OH). Neutravidin was obtained from PIERCE (Rockford, IL). Ni-NTA resin was obtained from GE healthcare (Amersham, UK).

4.2. General (chemistry)

All non-aqueous reactions were carried out using freshly distilled solvents under an atmosphere of argon. All reactions were monitored by TLC, which was carried out on Silica Gel 60 F254 plates (E. Merck, Darmstadt, Germany). Flash chromatography separations were performed on PSQ 100B (Fuji Silysia Co., Ltd, Japan).

The NMR spectra (^1H , ^{13}C) were determined on a Bruker 600 MHz or 400 MHz spectrometer (Avance DRX-600, Avance DRX-400) or a JEOL 400 MHz spectrometer (JNM-LD400), using CDCl_3 (with TMS for ^1H NMR and chloroform-*d* for ^{13}C NMR as the internal reference) solution, unless otherwise noted. Chemical shifts were expressed in parts per million (ppm) and coupling constants are in Hertz. Optical rotations were recorded on a JASCO P-1030 digital polarimeter using the sodium D line at room

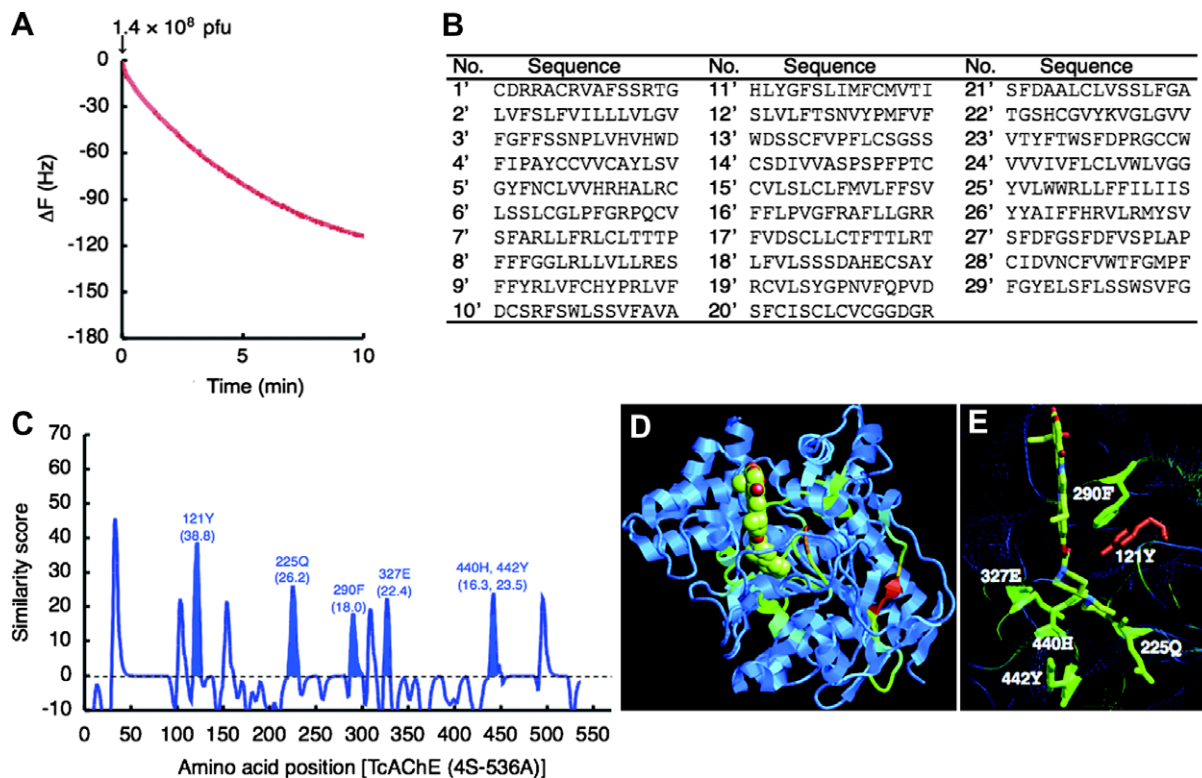


Figure 5. Detection of phage binding to Iri-SAM on the gold electrode after injection of a random-peptide T7 phage pool. Experiments were carried out according to the same procedure with SLF-SAM. (A) A representative sensorgram. (B) Iri-SAM-selected 15-mer peptide sequence after three sets of individual one-cycle screens. (C) Similarity scores for the sequence of TcAChE (4S-536A) against the sequences of peptides selected for affinity to Iri-SAM calculated using HETEROalign program in RELIC software. The similarity scores of random-peptides chosen without affinity selection (Supplementary Fig. 2) have been subtracted from these scores to remove pool bias. The maximal similarity score was observed for 121Y (38.8), 225Q (26.2), 290F (18.0), 327E (22.4), and 440H, 442Y (16.3 and 23.5) (highlighted in blue), which are involved in the Iri-binding site. (D) Three structural models of Iri-TcAChE complex (PDB ID: 1U65). The peptide backbone of AChE is shown in cartoon; Iri is shown in CPK. Oxygen and nitrogen in Iri are shown in red and cyan, respectively. Similarity is coded by color; red indicates the highest similarity and blue the lowest. (E) A close up view of the Iri-binding site rendered with RasMol with the amino-acid residues predicted to be involved in Iri-binding represented as a stick. Iri is shown in stick.

temperature, using CHCl_3 as a solvent unless otherwise noted. Infrared spectra (IR) were recorded on a Jasco FT/IR-410 spectrometer using NaCl (neat) or KBr pellets (solid), and were reported as wavenumbers (cm^{-1}). Mass spectra (MS) were obtained on an Applied Biosystems mass spectrometer (API QSTAR pulsar i) under conditions as high resolution, using polyethylene glycol as internal standard.

4.3. Synthesis of the SLF derivative that forms SAM

4.3.1. (1R)-3-(3,4-dimethoxyphenyl)-1-[3-(4-nitrophenoxycarbonyl-methoxy)phenyl]propyl (2S)-1-(3,3-dimethyl-2-oxovaleryl)-piperidine-2-carboxylate (SLF *p*-nitrophenyl ester, 2)

To a solution of **1** (172 mg, 0.29 mmol) and *p*-nitrophenol (52 mg, 0.37 mmol) in CH_2Cl_2 (5 ml) was added a solution of DCC (196 mg, 0.95 mmol) in CH_2Cl_2 (2 ml). Then, DMAP (43.2 mg, 0.35 mmol) was added to the mixture. The mixture was stirred at rt for 80 min and then concentrated. The residue was purified by silica gel chromatography (hexane/EtOAc = 4:1 to 2:1) to give **2** (194 mg, 94%) as a ca. 4:1 tautomeric mixture as yellow oil. $[\alpha]_D^{24} = -7.2$ ($c = 1.8$ in CHCl_3); $^1\text{H NMR}$ (600 MHz, CDCl_3 , major tautomer) $\delta = 8.27$ (2H, m), 7.33 (2H, m), 7.31 (1H, m), 7.03 (1H, d, $J = 7.7$ Hz), 7.00 (1H, br s), 6.93 (1H, dd, $J = 8.2$ Hz, 2.5 Hz), 6.77 (1H, m), 6.68 (2H, m), 5.80 (1H, dd, $J = 7.9$ Hz, 5.7 Hz), 5.32 (1H, br d, $J = 5.3$ Hz), 4.96 (2H, s), 3.85 (6H, s), 3.35 (1H, br d, $J = 12.7$ Hz), 3.16 (1H, td, $J = 13.1$ Hz, 2.9 Hz), 2.57 (2H, m), 2.36 (1H, m), 2.24 (1H, m), 2.07 (1H, m), 1.72 (5H, m), 1.45 (1H, m), 1.35 (2H, m), 1.22 (3H, s), 1.21 (3H, s), 0.88 (3H, t, $J = 7.4$ Hz); $^{13}\text{C NMR}$ (600 MHz, CDCl_3 , major tautomer) $\delta = 207.8, 169.7, 167.3,$

166.6, 157.7, 154.6, 148.9, 147.4, 145.6, 141.8, 133.3, 129.9, 125.3 (2 \times), 122.2 (2 \times), 120.4, 120.1, 114.6, 113.1, 111.7, 111.3, 76.4, 65.3, 55.9, 55.8, 51.2, 46.7, 44.1, 38.0, 32.4, 31.2, 26.3, 24.9, 23.4, 23.1, 21.1, 8.7; IR (neat) 3021, 2937, 2861, 1786, 1738, 1701, 1640, 1592, 1521, 1444, 1348, 1210, 1143, 1082, 1029, 992, 921, 864, 756 cm^{-1} ; HRMS (ESI) calcd for $\text{C}_{38}\text{H}_{44}\text{N}_2\text{O}_{11}$ $[\text{M}+\text{Na}]^+$: 727.2837, found 727.2800.

4.3.2. Bis{10-[11-(*N*-tert-butoxycarbonylamino)-3,6,9-trioxaundecylcarbamoyl]undecanyl} disulfide (5)

To a solution of **3** (221 mg, 0.75 mmol)²¹ in pyridine (3 ml) was added **4** (204 mg, 0.30 mmol)²² followed by DMAP (3.7 mg, 0.03 mmol) at rt. The mixture was stirred for 17 h. Then the mixture was quenched by the addition of H_2O and diluted with EtOAc. The layers were separated, and the organic layer was washed with brine and dried with Na_2SO_4 . After the organic layer was concentrated, the residue was purified by silica gel chromatography to yield **5** (249 mg, 84%) as a foam. $^1\text{H NMR}$ (600 MHz, CDCl_3) $\delta = 6.18$ (1H \times 2, br s), 5.03 (1H \times 2, br s), 3.64 (8H \times 2, br m), 3.56 (4H \times 2, m), 3.45 (2H \times 2, m), 3.32 (2H \times 2, m), 2.67 (2H \times 2, t, $J = 7.5$ Hz), 2.17 (2H \times 2, t, $J = 7.5$ Hz), 1.66 (4H \times 2, m), 1.45 (9H, s), 1.36 (2H \times 2, m), 1.26 (10H \times 2, br s); $^{13}\text{C NMR}$ (100 MHz, CDCl_3) $\delta = 173.3$ (2 \times), 156.0 (2 \times), 70.42 (2 \times), 70.39 (2 \times), 70.2 (2 \times), 70.14 (4 \times), 70.0 (2 \times), 40.3 (2 \times), 39.09 (2 \times), 39.06 (2 \times), 36.7 (2 \times), 29.41 (2 \times), 29.38 (2 \times), 29.32 (2 \times), 29.28 (2 \times), 29.17 (2 \times), 29.15 (2 \times), 28.5 (2 \times), 28.4 (6 \times), 25.7 (2 \times); IR (KBr) 3309, 3075, 2920, 2854, 1691, 1641, 1544, 1470, 1419, 1339, 1337, 1284, 1123, 1042, 868, 782, 758, 713 cm^{-1} ; HRMS (ESI) calcd for $\text{C}_{48}\text{H}_{94}\text{N}_4\text{O}_{12}\text{Na}_2\text{S}_2$ $[\text{M}+2\text{Na}]^{2+}$: 514.3135, found 514.3118.

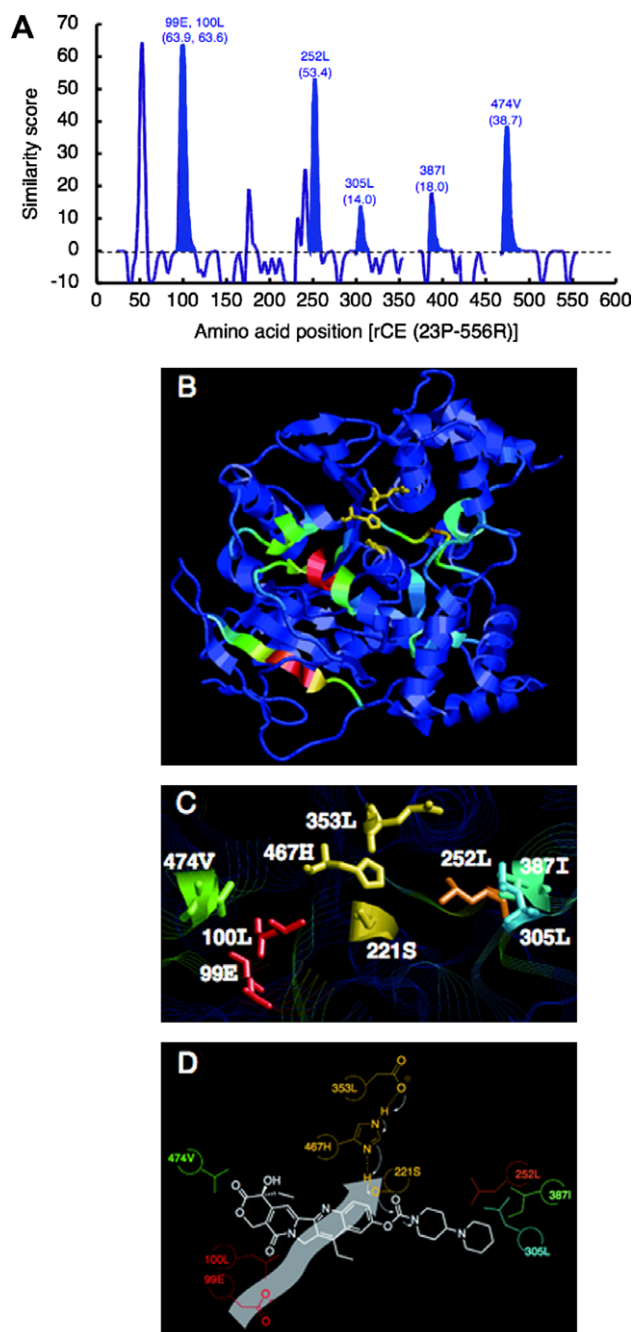


Figure 6. Analysis of interaction between Iri and rCE using a subset of Iri-SAM-selected peptides. (A) Similarity scores for the sequence of rCE (23P-556R) against the sequences of peptides selected for affinity to Iri-SAM (Fig. 5B) calculated using HETEROalign program in RELIC software. The similarity scores of random-peptides chosen without affinity selection (Supplementary Fig. 2) have been subtracted from these scores to remove pool bias. The maximal similarity score was observed for 99E, 100L (63.9 and 63.6), 252L (53.4), 305L (14.0), 387I (18.0), and 474V (38.7) (highlighted in blue), which are likely to be bound directly during the deesterification of Iri. (B) Three structural models of rCE (PDB ID: 1K4Y). The peptide backbone of CE is shown in cartoon. Similarity is coded by color; red indicates the highest similarity and blue the lowest. Amino-acid residues of the catalytic triad (221S, 353L, and 467H) are shown in yellow stick. (C) A close up view of the vicinity of the catalytic triad rendered with RasMol with the amino-acid residues predicted to be involved in Iri-binding represented as a stick. (D) Possible location of Iri (white) in CE during the deesterification. Gray arrow at the back shows part of beta strand (210G–220E), which was identified during our previous T7 phage display screen using CPT-10-B.

4.3.3. Bis[10-[(11-amino-3,6,9-trioxaundecanyl)carbamoyl]-undecanyl] disulfide, bistrifluoroacetic acid salt (**6**)

To a solution of **5** (20 mg, 0.02 mmol) in CH_2Cl_2 (2 ml) was added TFA (0.5 ml). The mixture was stirred at rt for 45 min and then con-

centrated. The resulting amine salt was used directly in the next step. ^1H NMR (600 MHz, CD_3OD) δ = 3.70 (2H \times 2, m), 3.68 (4H \times 2, br s), 3.65 (2H \times 2, m), 3.62 (2H \times 2, m), 3.53 (2H \times 2, t, J = 5.6 Hz), 3.35 (2H \times 2, t, J = 5.6 Hz), 3.13 (2H \times 2, brt, J = 4.9 Hz), 2.67 (2H \times 2, t, J = 7.3 Hz), 2.18 (2H \times 2, t, J = 7.3 Hz), 1.66 (2H \times 2, quintet, J = 7.3 Hz), 1.59 (2H \times 2, m), 1.39 (2H \times 2, m), 1.31 (10H \times 2, br s).

4.3.4. Bis(SLF-DEG-undecanyl) disulfide (**7**)

To a solution of **2** (58.4 mg, 0.076 mmol) in pyridine (3 ml) was added a solution of **6** (136.4 mg, 0.194 mmol) in CH_2Cl_2 (3 ml) at rt, and the mixture was stirred at rt for 7 h. Then the mixture was concentrated, and the residue was purified by silica gel chromatography to yield **7** (29.1 mg, 21%) as a ca. 4:1 tautomeric mixture in the form of a colorless oil. $[\alpha]_D^{24}$ = -3.6 (c = 0.67 in CHCl_3); ^1H NMR (600 MHz, CDCl_3 , major tautomer) δ = 7.31 (1H \times 2, t, J = 7.9 Hz), 7.05 (1H \times 2, brt, J = 5.6 Hz), 7.00 (1H \times 2, br d, J = 7.7 Hz), 6.93 (1H \times 2, br s), 6.86 (1H \times 2, dd, J = 7.9 Hz, 2.0 Hz), 6.78 (1H \times 2, m), 6.68 (1H \times 2, br s), 6.67 (2H \times 2, m), 6.09 (1H \times 2, br m), 5.77 (1H, dd, J = 7.9 Hz, 5.6 Hz), 5.31 (1H \times 2, d, J = 5.4 Hz), 4.50 (2H \times 2, s), 3.86 (3H \times 2, s), 3.85 (3H \times 2, s), 3.63 (8H \times 2, br s), 3.60 (2H \times 2, m), 3.57 (2H \times 2, m), 3.52 (2H \times 2, m), 3.44 (2H \times 2, m), 3.37 (1H \times 2, br d, J = 12.3 Hz), 3.18 (1H \times 2, td, J = 13.1 Hz, 2.9 Hz), 2.67 (2H \times 2, t, J = 7.4 Hz), 2.61 (1H \times 2, m), 2.53 (1H \times 2, m), 2.38 (1H \times 2, br d, J = 13.7 Hz), 2.25 (1H \times 2, m), 2.15 (2H \times 2, t, J = 7.4 Hz), 2.05 (1H \times 2, m), 1.80–1.60 (12H \times 2, m), 1.50 (1H \times 2, m), 1.35 (4H \times 2, m), 1.27 (10H \times 2, br s), 1.23 (3H \times 2, s), 1.21 (3H, s), 0.89 (3H \times 2, t, J = 7.4 Hz); ^{13}C NMR (100 MHz, CDCl_3 , major tautomer) δ = 207.8 (2 \times), 173.2 (2 \times), 169.7 (2 \times), 168.1 (2 \times), 167.3 (2 \times), 157.4 (2 \times), 148.9 (2 \times), 147.4 (2 \times), 141.9 (2 \times), 133.3 (2 \times), 130.0 (2 \times), 120.1 (2 \times), 120.1 (2 \times), 114.2 (2 \times), 113.3 (2 \times), 111.3 (2 \times), 76.5 (2 \times), 70.5 (4 \times), 70.3 (2 \times), 70.2 (2 \times), 70.0 (2 \times), 69.7 (2 \times), 67.4 (2 \times), 55.9 (2 \times), 55.8 (2 \times), 55.8 (2 \times), 51.3 (2 \times), 46.7 (2 \times), 44.1 (2 \times), 39.12 (2 \times), 39.10 (2 \times), 38.8 (2 \times), 36.7 (2 \times), 32.5 (2 \times), 31.2 (2 \times), 29.7 (2 \times), 29.5 (2 \times), 29.42 (2 \times), 29.36 (2 \times), 29.3 (2 \times), 29.21 (2 \times), 29.20 (2 \times), 28.5 (2 \times), 26.4 (2 \times), 25.7 (2 \times), 24.5 (2 \times), 23.5 (2 \times), 23.2 (2 \times), 21.2 (2 \times), 8.7 (2 \times); IR (neat) 3342, 2928, 2857, 1738, 1645, 1517, 1444, 1351, 1261, 1141, 1030, 992 cm^{-1} ; HRMS (ESI) calcd for $\text{C}_{102}\text{H}_{56}\text{N}_6\text{O}_{24}\text{Na}_2\text{S}_2$ $[\text{M}+2\text{Na}]^{2+}$: 979.5198, found 979.5220. calcd for $\text{C}_{102}\text{H}_{56}\text{N}_6\text{O}_{24}\text{NaS}_2$ $[\text{M}+\text{Na}]^+$: 1936.0504, found 1936.0549.

4.4. Synthesis of biotinylated SLF derivative (SLF-bio)

The SLF-bio was synthesized according to previous reports.^{13,14}

4.5. Synthesis of the Iri derivative that forms SAM

4.5.1. Bis[10-[(11-(4-nitrophenoxycarbonylamino)-3,6,9-trioxaundecanyl)carbamoyl]undecanyl] disulfide (**8**)

To a solution of **5** (81 mg, 0.082 mmol) in CH_2Cl_2 (1 ml) was added TFA (0.25 ml). The mixture was stirred at rt for 3.5 h and then concentrated. To a solution of the resulting ammonium salt in pyridine (1.2 ml) was added DMAP (1.6 mg, 0.013 mmol) and bis(4-nitrophenyl)carbonate (100 mg 0.33 mmol). The mixture was stirred at rt for 19 h and then concentrated, and the residue was purified by silica gel chromatography ($\text{CHCl}_3/\text{MeOH}$ = 50:1 to 25:1) to yield diester **8** (95 mg, quant) as a pale yellow crystal. ^1H NMR (400 MHz, CDCl_3) δ = 8.24 (2H \times 2, d, J = 9.3 Hz), 7.32 (2H \times 2, d, J = 7.3 Hz), 6.25–6.00 (2H \times 2, m), 3.90–3.32 (16H \times 2, m), 2.67 (2H \times 2, t, J = 7.3 Hz), 2.16 (2H \times 2, t, J = 7.7 Hz), 1.69–1.51 (4H \times 2, m), 1.49–1.20 (12H \times 2, m); HRMS (ESI) calcd for $\text{C}_{52}\text{H}_{84}\text{N}_6\text{O}_{16}\text{S}_2\text{Na}$ $[\text{M}+\text{Na}]^+$: 1135.5277, found 1135.5254.

4.5.2. 20-(*N*-Boc- β -alanyl) irinotecan (**10**)

To a solution of irinotecan (**9**) (51 mg, 0.075 mmol) in CH_2Cl_2 (9 ml) was added *N*-Boc- β -alanine (29 mg, 0.15 mmol). Then, 2-chloro-1-methylpyridium iodide (116 mg, 0.45 mmol) and DMAP

(92 mg, 0.75 mmol) was added to the mixture successively at 0 °C. The mixture was warmed and stirred at rt for 17 h and then concentrated. Then the mixture was quenched by the addition of 0.1 M HCl and diluted with CH₂Cl₂. The layers were separated, and the organic layer was washed with brine and dried with Na₂SO₄. After the organic layer was concentrated, the residue was purified by silica gel chromatography (CHCl₃/MeOH = 95:5 to 75:25) to yield **10** (35 mg, 61%) as a yellow crystal. $[\alpha]_D^{25} = -3.3$ ($c = 1.1$ in CHCl₃); ¹H NMR (400 MHz, CDCl₃) $\delta = 8.20$ (1H, d, $J = 9.3$ Hz), 7.84 (1H, d, $J = 2.4$ Hz), 7.60 (1H, dd, $J = 2.6$ Hz, 9.2 Hz), 7.17 (1H, s), 5.70 (1H, d, $J = 17.4$ Hz), 5.41 (1H, d, $J = 17.1$ Hz), 5.26 (2H, s), 5.21–5.18 (1H, m), 4.46–4.30 (2H, m), 3.65–3.35 (2H, m), 3.16 (2H, q, $J = 7.7$ Hz), 3.07 (1H, t, $J = 12.7$ Hz), 2.91 (1H, t, $J = 12.2$ Hz), 2.82–2.72 (1H, m), 2.80–2.50 (6H, m), 2.26 (1H, dq, $J = 7.1$ Hz, 14.7 Hz), 2.15 (1H, dq, $J = 7.1$ Hz, 14.7 Hz), 2.03–1.26 (22H, m), 1.00 (3H, t, $J = 7.6$ Hz); ¹³C NMR (100 MHz, CDCl₃) $\delta = 171.6$, 167.7, 157.4, 155.9, 153.1, 151.4, 150.5, 147.1, 147.0, 146.0, 145.43, 145.40, 131.6, 131.0, 127.6, 127.1, 127.0, 125.9, 119.6, 114.6, 95.7, 79.4, 77.3, 76.3, 67.2, 62.5, 50.2, 49.3, 44.3, 44.0, 36.4, 34.69, 34.67, 31.8, 31.6, 29.7, 28.4, 28.0, 27.3, 25.6, 25.3, 24.3, 23.2, 22.7, 20.7, 14.1, 14.0, 7.6; IR (neat) 1716, 1662, 1610 cm⁻¹; HRMS (ESI) calcd for C₄₁H₅₂N₅O₉ [M+H]⁺: 758.3765, found 758.3753.

4.5.3. 20-(β -alanyl) irinotecan ammonium salt (**11**)

To **10** (33 mg, 0.043 mmol) was added TFA (1.0 ml). The mixture was stirred at rt for 15 min and then concentrated. The resulting ammonium salt was used directly without further purification. $[\alpha]_D^{25} = -39.1$ ($c = 1.0$ in MeOH); ¹H NMR (400 MHz, CD₃OD) $\delta = 8.16$ (1H, d, $J = 9.0$ Hz), 8.02 (1H, d, $J = 2.4$ Hz), 7.68 (1H, dd, $J = 2.4$ Hz, 9.3 Hz), 7.37 (1H, s), 5.63 (1H, d, $J = 16.8$ Hz), 5.49 (1H, d, $J = 16.8$ Hz), 5.35 (2H, s), 4.58 (1H, br s), 4.39 (1H, br s), 3.65–2.97 (13H, m), 2.40–1.73 (11H, m), 1.56 (1H, m), 1.40 (3H, t, $J = 7.6$ Hz), 1.05 (3H, t, $J = 7.4$ Hz); ¹³C NMR (100 MHz, CD₃OD) $\delta = 171.3$, 169.3, 158.8, 154.5, 152.5, 151.6, 148.0, 147.8, 147.7, 147.6, 131.8, 130.0, 129.2, 128.7, 127.2, 120.3, 116.3, 97.6, 78.6, 67.8, 64.7, 58.3, 51.4, 50.7, 49.9, 44.3, 44.0, 36.1, 35.0, 33.0, 32.3, 31.9, 30.7, 30.5, 30.37, 30.34, 30.2, 27.6, 27.2, 26.8, 26.1, 25.3, 24.4, 23.9, 23.7, 22.9, 20.8, 18.4, 14.4, 14.3, 8.1; IR (neat) 1672, 1606 cm⁻¹; HRMS (ESI) calcd for C₃₆H₄₄N₅O₇ [M+H]⁺: 658.3240, found 658.3221.

4.5.4. Bis[20-(β -alanyl) irinotecan]-DEG-undecanyl disulfide (**12**)

To a solution of **11** (6.4 mg, 0.0083 mmol) in pyridine (0.5 ml) and CH₂Cl₂ (0.1 ml) was added **8** (4.0 mg, 0.0036 mmol) at rt, and the mixture was stirred at rt to 40 °C for 3 days. Then the mixture was concentrated, and the residue was purified by silica gel chromatography (CHCl₃/MeOH = 95:5 to 2:1) to yield **12** (4.8 mg, 62%) as a yellow crystal. $[\alpha]_D^{25} = -8.6$ ($c = 0.45$ in MeOH); ¹H NMR (400 MHz, CD₃OD) $\delta = 8.11$ (1H \times 2, d, $J = 9.0$ Hz), 7.89 (1H \times 2, d, $J = 0.96$ Hz), 7.56 (1H \times 2, dd, $J = 9.3$ Hz, 0.96 Hz), 7.31 (1H \times 2, s), 5.61 (1H \times 2, d, $J = 16.6$ Hz), 5.46 (1H \times 2, d, $J = 16.6$ Hz), 5.23 (2H \times 2, s), 4.58 (1H \times 2, br s), 4.39 (1H \times 2, br s), 3.75–3.08 (26H \times 2, m), 3.08–2.95 (1H \times 2, m), 2.92–2.72 (2H \times 2, m), 2.72–2.56 (2H \times 2, m), 2.30–1.15 (33H \times 2, m), 1.03 (3H \times 2, t, $J = 7.5$ Hz); ¹³C NMR (100 MHz, CD₃OD) $\delta = 176.4$, 172.7, 169.4, 160.8, 158.92, 158.87, 154.5, 151.7, 148.4, 148.0, 147.9, 133.5, 132.4, 132.3, 132.0, 130.1, 129.9, 127.0, 120.3, 116.5, 97.9, 77.8, 67.7, 67.3, 66.9, 64.8, 58.3, 51.4, 50.8, 44.4, 44.2, 44.0, 41.0, 40.3, 39.8, 37.1, 36.9, 35.7, 33.0, 32.0, 30.7, 30.5, 30.4, 30.4, 30.2, 30.1, 29.6, 29.4, 27.0, 26.9, 25.4, 24.5, 23.9, 23.7, 22.9, 18.4, 14.3, 8.2; IR (neat) 1682, 1435 cm⁻¹; HRMS (ESI) calcd for C₁₁₂H₁₆₄N₁₄O₂₄S₂ [M+4H]²⁺: 1076.5736, found 1076.5771.

4.6. Construction of a natural-protein T7 phage pool

A natural-protein T7 phage pool was constructed using Jurkat cell-derived cDNA according to the manufacturer's instructions.^{16,23} The primary titer of this T7 phage pool was 5.8×10^6 pfu/ml. For

the screening procedure, the phage pool was amplified up to 1.0×10^{10} pfu/ml using *E. coli* (BLT5615) as the host strain.

4.7. Construction of the T7 phage pool using synthetic DNA

For the preparation of a duplex DNA library, oligonucleotide GGGGATCCGAATTCT(NNK)₁₅TGAAAGCTTCTCGAGGG (0.056 μ M) and CCCTCGAGAAGCTTTCA (0.56 μ M) were mixed with Klenow buffer, heated to 95 °C for 5 min and annealed by cooling the mixture to 37 °C. The single-stranded regions were converted to duplex DNA by continuing the incubation at 37 °C for 2 h in the presence of dNTPs (2.5 mM) and Klenow enzyme (0.5 mU/ μ l). After the reaction, double-stranded DNA was recovered by EtOH precipitation. The obtained DNA was then digested separately with EcoRI and HindIII restriction enzyme and inserted into the T7select10-3b vector according to the manufacturer's instructions.^{16,23} The primary titer of this T7 phage pool was 1.6×10^7 pfu/ml. For the screening procedure, the phage pool was amplified up to 1.7×10^{10} pfu/ml using *E. coli* (BLT5615) as the host strain.

4.8. Expression of Six Histidine-tagged FK506-binding protein 12 (FKBP12)

The cDNA encoding human FKBP12 was cloned into the expression vector pET28a(+) (Novagen), and the *E. coli* BL21(DE3) was transformed with the vector. A single colony was inoculated into 15 ml of LB medium containing 1% glucose and 50 μ g/ml of kanamycin and cultured at 30 °C. The cells were grown overnight and then used to inoculate another 1000 ml of the same medium at 37 °C. After 3 h of growth, heterologous expression of FKBP12 was induced by addition of 1 mM of IPTG. The culture was then continued for a further 3 h at 37 °C. The cultured cells were harvested by centrifugation at 1500g for 10 min at 4 °C. The cells were resuspended in PBS and centrifuged at 1100g for 10 min at 4 °C. After removing the supernatant, the cell paste was frozen using liquid nitrogen and then stored at –80 °C until use.

4.9. Purification of His-tagged FKBP12

The FKBP12-producing cells were sonicated in buffer A (50 mM phosphate, pH 8.0, 300 mM NaCl, 10 mM imidazole (Im), 1 mM phenylmethylsulfonyl fluoride (PMSF), 1 μ g/ml leupeptin) and then centrifuged for 30 min at 20,400g at 4 °C. The supernatant was filtered using a PVDF membrane (Milllex, pore size 0.45 μ m, Millipore, Billerica, MA) and then loaded onto a Ni-NTA resin (GE healthcare) pre-equilibrated with buffer A. The column was washed in turn with buffer B (50 mM phosphate, pH 8.0, 300 mM NaCl, 20 mM Im), buffer C (50 mM phosphate, pH 8.0, 300 mM NaCl, 30 mM Im) and buffer D (50 mM phosphate, pH 8.0, 300 mM NaCl, 40 mM Im). Bound proteins were then eluted with buffer E (50 mM phosphate, pH 8.0, 300 mM NaCl, 250 mM Im). The fractions containing the His-tagged FKBP12 were collected and dialyzed into TEMG buffer (50 mM Tris-HCl, pH 7.5, 1 mM EDTA, 50 mM NaCl, 10% (v/v) glycerol, 5 mM 2-mercaptoethanol) for the following purification by FPLC. The protein was loaded onto HiTrap DEAE column pre-equilibrated with TEMG buffer, and the flow-through fraction was then subjected to HiTrap SP column chromatography. The flow-through fraction was collected and dialyzed into FKBP buffer (25 mM Tris-HCl, pH 7.5, 50 mM NaCl, 1 mM MgCl₂, 1 mM CaCl₂, 10% (v/v) glycerol, 5 mM 2-mercaptoethanol, 0.05% (v/v) Nonidet P-40) and then stored at –80 °C until use.

4.10. Procedure for the T7 phage display screen using a cuvette type QCM apparatus

A 20 μ l aliquot of SLF derivative (**7**) (1.3 mM in 75% EtOH) or Iri derivative (**12**) (1 mM in 75% EtOH) was dropped onto the gold elec-

trode of the ceramic sensor chip and left for 16 h under a humid and shaded atmosphere at room temperature. The surface of the electrode was washed for 10 min in buffer (10 mM Tris–HCl, pH 8.0, 200 mM NaCl), which was stirred at 1000 rpm. The sensor chip was setup for the QCM apparatus with the cuvette containing 8 ml of buffer. The QCM sensor was then allowed to fully stabilize. An aliquot of 8 μ l of His-tagged FKBP12 (2, 4, 8, 17, 33, and 67 μ M), 16 μ l of natural-protein T7 phage pool (1.0×10^{10} pfu/ml) and 8 μ l of random-peptide T7 phage pool (1.7×10^{10} pfu/ml) were individually injected into the cuvette. Frequency changes, caused by binding to the SLF immobilized on the gold electrode surface, were then monitored for 10 min. For the recovery of bound phages, 10 μ l of host *E. coli* (BLT5615) solution (cultured for 30 min at 37 °C in the presence of 1 mM of IPTG beforehand) was dropped onto the gold electrode and then incubated at 37 °C for 30 min. To the resulting solution was then added another 200 μ l of LB medium. An aliquot of phage was then extracted from this solution and subjected to PCR analysis followed by agarose gel electrophoresis and DNA sequencing.

For SLF-bio immobilization, the gold sensor surface was initially coated by treatment with 100 μ l of neutravidin solution (100 μ g/ml aq) for 30 min at room temperature. After washing the gold electrode surface, SLF-bio was applied and left for 16 h under a humid and shaded atmosphere at room temperature. The gold surface was thoroughly washed prior to conducting the screening experiments.

4.11. Agarose gel electrophoresis and DNA sequencing

Agarose gel electrophoresis and DNA sequencing were performed as described previously.⁴

4.12. RELIC software

RELIC software (<http://relic.bio.anl.gov/index.aspx>) was used for the screening with the T7 phage pool constructed from synthetic DNA according to the supplier's manuals.⁹

Acknowledgments

We thank Yakult Co. Ltd (Tokyo, Japan) and Dai-ichi Pharmaceutical Co. Ltd (Tokyo, Japan) for providing irinotecan. This work was partially supported by a Grant-in-Aid for Scientific Research (The Ministry of Education, Culture, Sports, Science and Technology of Japan, Japan Society for the Promotion of Science)

Supporting information available

Additional experimental details. This material is available free of charge via the Internet at <http://www.Xxx.xxxx>. Supplementary data associated with this article can be found, in the online version, at doi:10.1016/j.bmc.2008.09.061.

References and notes

- Rodi, D. J.; Agoston, G. E.; Manon, R.; Lapcevic, R.; Green, S. J.; Makowski, L. *Comb. Chem. High Throughput Screen.* **2001**, *4*, 553.
- Rodi, D. J.; Janes, R. W.; Sanganee, H. J.; Holton, R. A.; Wallace, B. A.; Makowski, L. *J. Mol. Biol.* **1999**, *285*, 197.
- Smith, G. P.; Petrenko, V. A. *Chem. Rev.* **1997**, *97*, 391.
- Takakusagi, Y.; Takakusagi, K.; Kuramochi, K.; Kobayashi, S.; Sugawara, F.; Sakaguchi, K. *Bioorg. Med. Chem.* **2007**, *15*, 7590.
- Takakusagi, Y.; Kuroiwa, Y.; Sugawara, F.; Sakaguchi, K. *Bioorg. Med. Chem.* **2008**, *16*, 7410.
- Love, J. C.; Estroff, L. A.; Kriebel, J. K.; Nuzzo, R. G.; Whitesides, G. M. *Chem. Rev.* **2005**, *105*, 1103.
- Holt, D. A.; Luengo, J. I.; Yamashita, D. S.; Oh, H.; Konialian, A. L.; Yen, H.; Rozamus, L. W.; Brandt, M.; Bossard, M. J.; Levy, M. A.; Eggleston, D. S.; Liang, J.; Schultz, L. W.; Stout, T. J.; Clardy, J. *J. Am. Chem. Soc.* **1993**, *115*, 9925.
- Garcia-Carbonero, R.; Supko, J. G. *Clin. Cancer Res.* **2002**, *8*, 641.
- Mandava, S.; Makowski, L.; Devarapalli, S.; Uzubell, J.; Rodi, D. J. *Proteomics* **2004**, *4*, 1439.
- Rodi, D. J.; Makowski, L. *Pac. Symp. Biocomput.* **1999**, *4*, 532.
- Furuya, M.; Haramura, M.; Tanaka, A. *Bioorg. Med. Chem.* **2006**, *14*, 537.
- Clackson, T.; Yang, W.; Rozamus, L. W.; Hatada, M.; Amara, J. F.; Rollins, C. T.; Stevenson, L. F.; Magari, S. R.; Wood, S. A.; Courage, N. L.; Lu, X.; Cerasoli, F. J.; Gilman, M.; Holt, D. A. *Proc. Natl. Acad. Sci. U.S.A.* **1998**, *95*, 10437.
- Keenan, T.; Yaeger, D. R.; Courage, N. L.; Rollins, C. T.; Pavone, M. E.; Rivera, V. M.; Yang, W.; Guo, T.; Amara, J. F.; Clackson, T.; Gilman, M.; Holt, D. A. *Bioorg. Med. Chem.* **1998**, *6*, 1309.
- McKenzie, K. M.; Vidlock, E. J.; Splittgerber, U.; Austin, D. J. *Angew. Chem. Int. Ed. Engl.* **2004**, *43*, 4052.
- Bain, C. D.; Troughton, E. B.; Tao, Y.; Evall, J.; Whitesides, G. M.; Nuzzo, R. G. *J. Am. Chem. Soc.* **1989**, *111*, 321.
- Novagen. OrientExpress™ cDNA Manual, 1999, TB247.
- Yang, W.; Rozamus, L. W.; Narula, S.; Rollins, C. T.; Yuan, R.; Andrade, L. J.; Ram, M. K.; Phillips, T. B.; van Schravendijk, M. R.; Dalgarno, D.; Clackson, T.; Holt, D. A. *J. Med. Chem.* **2000**, *43*, 1135.
- Yoon, K. J.; Hyatt, J. L.; Morton, C. L.; Lee, R. E.; Potter, P. M.; Danks, M. K. *Mol. Cancer Ther.* **2004**, *3*, 903.
- Harel, M.; Hyatt, J. L.; Brumshtein, B.; Morton, C. L.; Yoon, K. J.; Wadkins, R. M.; Silman, I.; Sussman, J. L.; Potter, P. M. *Mol. Pharmacol.* **2005**, *67*, 1874.
- Bencharit, S.; Morton, C. L.; Howard-Williams, E. L.; Danks, M. K.; Potter, P. M.; Redinbo, M. R. *Nat. Struct. Biol.* **2002**, *9*, 337.
- Belser, T.; Stöhr, M.; Pfaltz, A. *J. Am. Chem. Soc.* **2005**, *127*, 8720.
- Zhang, W.; Nowlan, D. T. r.; Thomson, L. M.; Lackowski, W. M.; Simanek, E. E. *J. Am. Chem. Soc.* **2001**, *123*, 8914.
- Novagen. T7Select® System Manual, 2000, TB178.